

Central neurotoxicity induced by the instillation of ZnO and TiO₂ nanoparticles through the taste nerve pathway

Aim: To explore whether nanoparticles (NPs) can be transported into the CNS via the taste nerve pathway. **Materials & methods:** ZnO and TiO₂ NPs were tongue-instilled to male Wistar rats. Toxicity was assessed by Zn/Ti biodistribution, histopathological examination, oxidative stress assay, quantitative reverse-transcriptase PCR analysis, learning and memory capabilities. **Results:** ZnO NPs and TiO₂ NPs significantly deposited in the nerves and brain, respectively. The histopathological examination indicated a slight injury in the cerebral cortex and hippocampus. Ultrastructural changes and an imbalanced oxidative stress were observed. The Morris water maze results showed that the learning and memory of rats were impaired. **Conclusion:** NPs can enter the CNS via the taste nerve translocation pathway and induce a certain adverse effect.

First draft submitted: 11 May 2017; Accepted for publication: 14 August 2017; Published online: 20 September 2017

Keywords: learning and memory • neurotoxicity • oxidative stress • taste nerve • TiO₂ nanoparticle • ZnO nanoparticle

Nanomaterials are defined as materials with at least one dimension in the range of 1–100 nm [1]. Because of their unique size, large surface area and high bioactivity, nanoparticles (NPs) have found wide application in numerous fields, including physics, materials science, biology and medicine. Therefore, the risk of exposure of the human body to NPs through inhalation [2,3], ingestion [4] and skin contact [5] is increasing. Following uptake, NPs can be transported to secondary target organs, especially the brain, resulting in potential damage to the CNS and neurotoxicity [6].

Surface modifications can allow NPs to circumvent or cross the blood–brain barrier (BBB), and NPs therefore hold great promise in medicine. Recently, evidence indicated that NPs can cause severe central neurotoxicity in animals. For instance, it had been found that learning and memory ability in rats could be impaired by ZnO NPs [7]. TiO₂ NPs were found to deposit in the hip-

pocampus, resulting in hippocampus apoptosis and dysfunction [8]. NPs are small and can easily enter the brain and be taken up by brain cells such as neurons and glial cells. The mechanism of cellular uptake of NPs mainly includes macropinocytosis, endocytosis mediated by clathrin or caveolae and endocytosis without clathrin or caveolae [9].

In addition, NPs can be transported along nerves. Evidence indicates that neural connections to the nasal passages of the brain and spinal cord contribute to the transport of NPs absorbed into the nasal mucosa to the CNS [10]. In addition, NPs that pass the olfactory epithelium can be transferred to the CNS via the trigeminal nerve [11,12].

At present, ZnO NPs and TiO₂ NPs are among the most common nanomaterials and are mainly used in cosmetics [13] and biomedicine [14]. Notably, they are often used as food supplements, such as in chewing gums, candies and toothpastes [15–17], which allow the possibility of NPs entering the body through

Chen Aijie¹, Liang Huimin¹,
Liu Jia¹, Ou Lingling², Wei
Limin³, Wu Junrong¹, Lai
Xuan¹, Han Xue⁴ & Shao
Longquan^{*1}

¹Nanfang Hospital, Southern Medical University, Guangzhou 510515, China

²The First Affiliated Hospital, Jinan University, Guangzhou 510630, China

³School & Hospital of Stomatology, Wenzhou Medical University, Wenzhou 325027, China

⁴The 309th Hospital of Chinese People's Liberation Army, Beijing 100091, China

*Author for correspondence:

Tel.: +86 15989283921

shaolongquan@smu.edu.cn

the taste nerve. Similar to the olfactory receptor system, the taste receptors are capable of recognizing the characteristics of different foods and transmit sensory signals to the brain [18–20]. According to reports, humans typically have 5000–10,000 taste buds, most of which are located in the tongue, palate and epiglottis [21,22]. Each taste bud consists of a group of 50–100 neuro-epithelial cells contained in the oral epithelium [21–23]. These cells have unique functions that can be linked to neurons, transforming taste stimuli (sweet, bitter, salty, sour, umami) into electrochemical signals to sensory nerves [24]. They also play an important role in terminating synaptic transmission, and support cells such as glial cells in the taste buds [21]. The glossopharyngeal nerve conveys afferent information from the taste buds on the posterior third of the tongue, and the chorda tympani (CT) is the branch of the afferent facial nerve that conveys sensory information from the anterior two thirds of the tongue [25]. Taste information is conveyed via the facial and glossopharyngeal nerves [26] to the medulla nucleus of the solitary tract (NST) [27,28], parabrachial nucleus [29,30], posterior thalamic nucleus [31] and finally to the insular cortex, which is the destination of afferent taste signals and visceral sensory signals [32]. It has been reported that the dorsal mid-insula regions show a corresponding gustatory response following interoception measured by functional MRI, indicating that neurons in dorsal mid-insula can receive gustatory stimulation [33]. Thus, it is very possible for NPs to be taken up by the cells in the taste buds, enter afferent taste fibers, be transported along taste nerves such as the CT or glossopharyngeal nerves, and then transferred to the NST, parabrachial nucleus, posterior thalamic nucleus, ultimately accumulating in the gustatory cortex of the insula after exposure to tongue instillation (Figure 1).

Identification of the NP transport route into the body is essential to evaluate central neurotoxicity. The previous study showed that the main route for nerve translocation of NPs is the olfactory pathway [34,35]. In addition, the taste nerve is also an important sensory nerve and has similarities to the olfactory nerve. NPs have been suggested to be translocated into the CNS through the taste nerve pathway. However, there has been no study on whether NPs can be transported through the taste nerve and the potential effects on the CNS. Consequently, the present study explored whether and where NPs are translocated into the brain via the taste nerve and evaluated the central neurotoxicity of ZnO NPs and TiO₂ NPs.

Material & methods

Characterization of ZnO & TiO₂ NPs

Powder-form ZnO and TiO₂ NPs were obtained from Sigma-Aldrich (USA). The primary particle sizes and

morphology were measured using transmission electron microscopy (TEM; JEOL, Tokyo, Japan). The compositions of the NPs were measured by energy dispersive spectroscopy (SwiftED3000, Tokyo, Japan). The hydrodynamic size and zeta potentials of the NPs in distilled water (DW) were determined through dynamic light scattering (DLS) performed on a Zetasizer Nano ZS instrument (Malvern, Malvern, UK), according to the manufacturer's instructions. Additionally, the specific surface areas of the NPs were measured through N₂ adsorption–desorption Brunauer–Emmett–Teller adsorption analysis on a Micromeritics ASAP 2010M+ C instrument (Micromeritics Co., GA, USA). Levels of endotoxin contamination were measured using an E-Toxate Kit (Sigma-Aldrich, MO, USA).

Animals & experimental design

Healthy Wistar male rats, 4–6 weeks old and 130–150 g in body weight (BW), were purchased from the Animal Center of Southern Medical University (Guangzhou, China). The animals were placed in a sterile room (23 ± 1°C room temperature, 60 ± 10% relative humidity) for a 12-h light/dark cycle and adapted to this environment for 5 days before treatment. All procedures used in this experiment were approved by the National Animal Ethics Committee of China. The approval number provided by the Southern Medical University ethical committee was 2015-021.

The rats were randomly allocated into three groups with comparable weights: the control, ZnO NPs and TiO₂ NPs groups. ZnO NPs and TiO₂ NPs were dispersed in DW, sonicated for 30 min and vortexed for 3 min before the tongue instillation. In the studies of ZnO NPs and TiO₂ NPs toxicity, oral administration is one of the most common exposures. We referred to the doses of oral administration in other animal models [36–38], and finally choose a relatively low dose (50 mg/kg). Rats were weighed and anesthetized by an intraperitoneal injection of 1% pentobarbital sodium (48 mg/kg). The rats were held in lateral position, and the tongue was pulled out from the corner of the mouth. Then, a microsyringe with a suspension of 50 mg/ml ZnO NPs and TiO₂ NPs (50 mg/kg BW per mouse) was instilled to the surface of the tongue drop by drop, ensuring the NPs had been contacted with the whole tongue. The instillation procedure lasted about an hour. After instillation, the tongue was rinsed with DW repeatedly until no suspension residue remained. The control group was instilled with an equal amount of DW. This anesthetization and instillation procedure was performed every other day for 30 days.

The animals were sacrificed at 24 h (30 days) after the last exposure, and the tissues, including the brain (cerebellum, brainstem, cerebral cortex and hippocam-

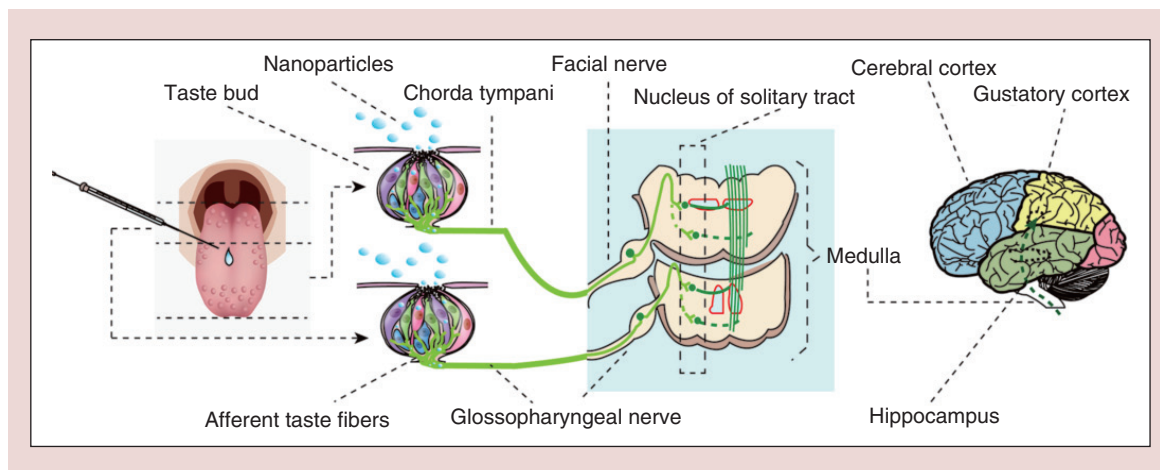


Figure 1. The pathway for the translocation of nanoparticles (ZnO and TiO₂) to the brain by tongue instillation.

pus), nerves (CT and glossopharyngeal nerve), heart, liver, spleen, kidneys, lung and blood, were extracted to examine Zn content and Ti content ($n = 6$), perform TEM and real-time quantitative reverse-transcriptase-PCR (qRT-PCR; $n = 6$), analyze oxidative stress ($n = 6$) and perform pathological and immunohistochemical examinations ($n = 6$). Rats were evaluated in the Morris water maze (MWM) test after exposure ($n = 6$). A total of 90 rats were used in the study.

Determination of Zn content & Ti content

The frozen brain, nerves (CT and glossopharyngeal nerve), heart, liver, spleen, kidneys, lung and blood were digested using concentrated nitric acid (ultrapure grade) and H₂O₂. Inductively coupled plasma-MS (Thermo Fisher Scientific, MA, USA) was used to quantify the Zn and Ti concentrations in each sample. We used calibration standards of 0.05, 0.1, 0.2, 0.4, 0.6 and 0.8 mg/l Zn and Ti to validate the method.

Transmission electron microscopy

Small blocks (~1 mm³) of brain tissue ($n = 6$) were fixed for 2 h. Then, the samples were dehydrated through an ethanol gradient and embedded in Epon resin. Finally, ultrathin tissue sections (500 nm) were mounted on grids. The brain tissue of the cerebral cortex is taken from the gustatory cortex. Ultrastructural examination and photography were performed with an H-7500 transmission electron microscope (Hitachi, Toyko, Japan).

Oxidative stress in the CNS

Six brain tissues of each group were weighed, chopped and put into a centrifuge tube. The homogenate (1:9 w/v) was centrifuged at 2500 r/min for 10 min at 4°C. After centrifugation, the supernatant was diluted in phosphate-buffered saline according to recommenda-

tions. Oxidative stress markers (SOD, MDA, GSH, GSH-Px and GSH/GSSG) were identified using a commercial colorimetric assay kit (Nanjing Jiancheng Bioengineering Institute, Jiangsu, China) in accordance with the manufacturer's protocols. The protein content was measured using Coomassie Blue staining.

Gene expression by quantitative real-time PCR

The brain samples were removed and maintained at -80°C after the rats were sacrificed. The frozen tissues were homogenized and extracted using TRIzol reagent (Gibco, MA, USA) in accordance with the manufacturer's instructions ($n = 6$). Synthesized complementary DNA was prepared using the PrimeScript™ RT reagent kit (TaKaRa, Shiga, Japan). qRT-PCR was conducted using a commercial kit (SYBR Premix Ex Taq II, TaKaRa, Shiga, Japan) and analyzed on a LightCycler 480 Sequence Detector System (Roche, Basel, Switzerland).

The primer sequences for oxidative stress-related genes (7-dehydrocholesterol reductase [*Dhcr7*]; CYP450, family 51 [*Cyp51*]; glutathione-disulfide reductase [*Gsr*]; NADPH oxidase 1 [*Nox1*]; superoxide dismutase 2, mitochondrial [*Sod2*]; NAD(P)H quinone dehydrogenase 1 [*Nqo1*]; flavin-containing monooxygenase 2 [*Fmo2*]) and learning and memory-related genes (serum/glucocorticoid-regulated kinase 1 [*Sgk1*]; dopamine receptor D2 [*Drd2*]; trafficking protein particle complex 4 [*Trappc4*]; guanine nucleotide-binding protein, α -q polypeptide [*Gnap*]) are shown in Tables 1 & 2.

Pathological examination

After exposure for 30 days, brain tissues ($n = 6$) were excised, washed with 0.9% cold saline and fixed in 10% buffered formalin overnight. Briefly, the samples were dehydrated in ethanol and xylene solutions, embedded

Table 1. Oxidative stress-related genes and primer sequences for quantitative reverse-transcriptase-PCR.

Gene name		Primer sequence (5'-3')
Dhcr7	Forward	TTCAAAGTCCCAGCACAA
	Reverse	AAGCGTTCACAAACCAGA
Cyp51	Forward	CTTAGCCTTGCTACCTGTT
	Reverse	ACCTCTTCCGCATTCA
Gsr	Forward	TCTTCAGCCACCCGCCAT
	Reverse	TGGATGCCAACCACCTCT
Nox1	Forward	TTTCCTAAACTACCGACTC
	Reverse	TGCGACAAACGGACTATC
Sod2	Forward	CCTGACCTGCTTACGACT
	Reverse	GCGACCTTGCTCCTTATTG
Nqo1	Forward	CATCATTGGGCAAGTCC
	Reverse	CACAGCCGTGGCAGAAC
Fmo2	Forward	CCTGGAAGACTCGCTTGT
	Reverse	AGGCTGGATGAGACCTATGC
β -actin	Forward	TGAAGTACCCATTGAACACGG
	Reverse	GGGTCATCTTTCACGGTTGG

in paraffin blocks and sliced at a thickness of 4 μ m using a microtome. After hematoxylin-eosin staining, pathological changes were observed with a digital camera integrated with a light microscope (Olympus, Tokyo, Japan).

Immunohistochemistry method

Immunohistochemistry was performed to identify the specific neurotoxicity effects. The presence of proliferating cells and apoptotic cells in brain sections was analyzed using Ki-67 immunoreactivity (Abcam, MA, USA). The oxidative damage to nucleic acids of brain cells was analyzed by 8-hydroxy-2-deoxyguano-

sine (8-OHdG) immunohistochemistry (Japan Institute for the Control of Aging, Shizuoka, Japan). The activation of astrocytes was detected by glial fibrillary acidic protein (GFAP; CST, MA, USA) immunohistochemical staining. Photographs of positive staining (brown) were captured at randomly selected fields in both the cortex and hippocampus and counted by the software Image J.

MWM test

To evaluate the impact of ZnO NPs and TiO₂ NPs on spatial learning and memory, male rats ($n = 6$) underwent the MWM test after tongue instillation for 30 days. The maze, filled with water (2.0 m diameter, 0.8 m high), was divided into four quadrants with an escape platform (10 cm diameter) placed approximately 2 cm below the surface of opaque water ($25 \pm 1^\circ\text{C}$). Visible cues were placed around the water maze.

During the 5-day training sessions, rats underwent four trials in different quadrants. They were required to find the escape platform in 90 s. On the sixth day (probe trial), rats were placed at the opposite side to swim for 60 s. On the seventh and eighth days, reverse escape platform training (reacquisition trials) was performed as described for the acquisition trial. Throughout the training and testing, parameters in the MWM such as the latency to reach the platform, the swimming speed and swimming distance were recorded automatically by a ceiling-mounted tracking system.

Statistical analysis

All results are expressed as mean \pm SEM. An analysis of variance with repeated measures was applied in the MWM test, and unpaired Student's t-tests were used for the other comparisons between two groups. All analyzes were performed in SPSS 19.0 software. A p-value of <0.05 was considered statistically significant.

Results

Physicochemical characterization of NPs

The ZnO NPs were hexagonal (Figure 2A), and the TiO₂ NPs were spherical (Figure 2D). The primary size of the ZnO NPs measured by TEM was 50 nm, and the primary size of the TiO₂ NPs was 25 nm. The peak values of ZnO NPs (Figure 2B) and TiO₂ NPs (Figure 2E) in x-ray diffraction analysis were consistent with the standard. The hydrodynamic diameters of the particles as determined by DLS were 450.6 for ZnO NPs (Figure 2C) and 209.5 for TiO₂ NPs (Figure 2F). The surface area of the ZnO NPs was 32.17 m²/g, while the TiO₂ NPs exhibited a larger surface area of 96.32 m²/g. In addition, the zeta potential of the ZnO NPs was 32.9 mV at pH 7.0, whereas the zeta potential of the TiO₂ NPs was 10.8 mV. No endotoxin contami-

Table 2. Learning and memory-related genes and primer sequences for quantitative reverse-transcriptase-PCR.

Gene name		Primer sequence (5'-3')
Sgk1	Forward	GAGCACAAATGGGACAACG
	Reverse	TCAAAGTGGCGAACGGTCA
Drd2	Forward	GTAATGCCGTGGGTTGTC
	Reverse	CTGTATTGTTGAGTCGAAAGA
Trappc4	Forward	CTGGACCTACTGCTGAAAC
	Reverse	AAAGAGCGAGTGGAACAT
Gnap	Forward	TATGTAGACGCAATAAGAGC
	Reverse	GTAGGCAGATAGGAAGGGT
β -actin	Forward	TGAAGTACCCATTGAACACGG
	Reverse	GGGTCATCTTTCACGGTTGG

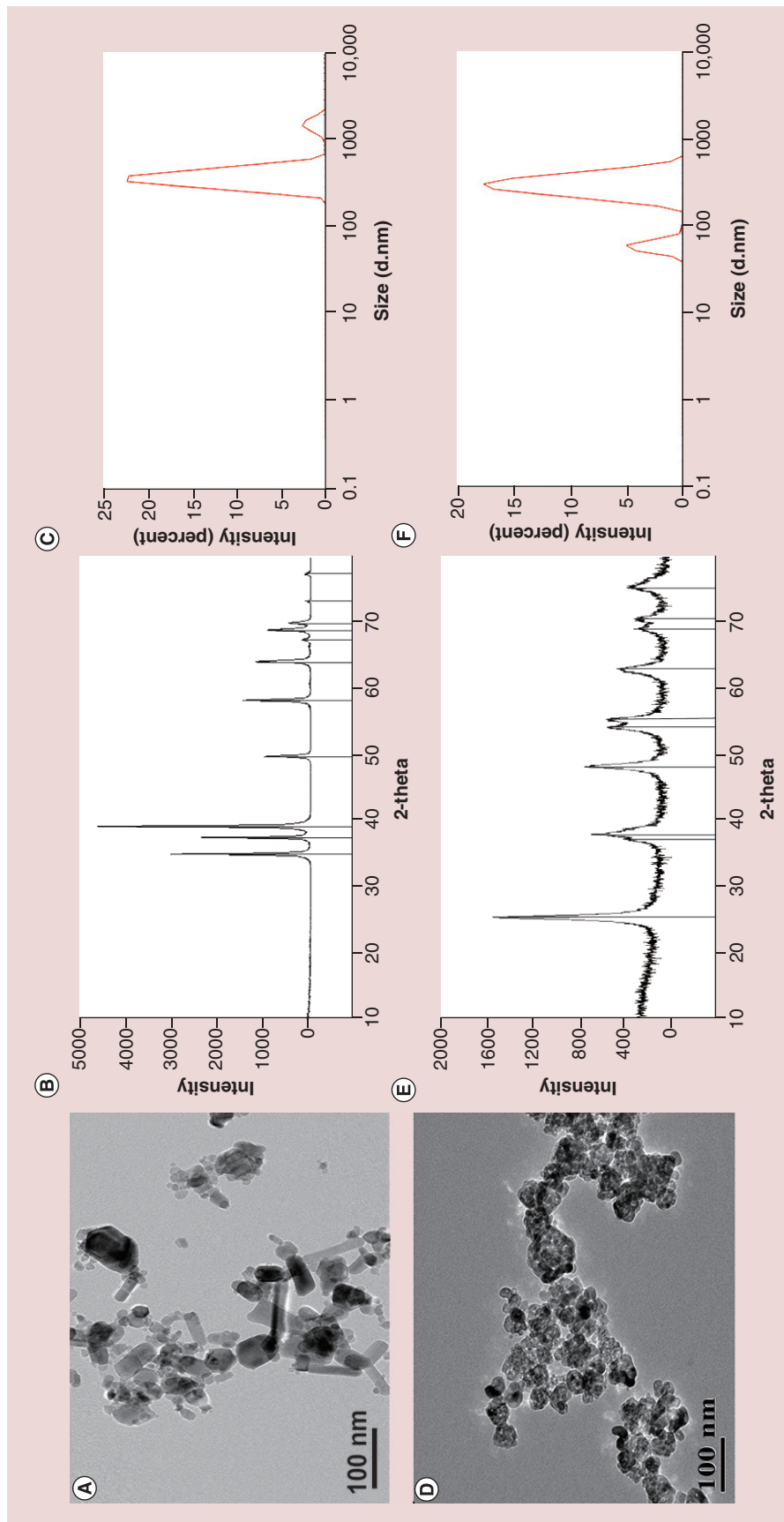


Figure 2. Characterization of ZnO and TiO₂ nanoparticles. (A) TEM image of ZnO NPs revealing a hexagonal shape. (B) XRD pattern of ZnO NPs. (C) Hydrodynamic size of ZnO NPs dispersed in DW as measured by DLS. (D) TEM image of TiO₂ NPs showing a spherical shape. (E) XRD pattern of TiO₂ NPs. (F) Hydrodynamic size of TiO₂ NPs dispersed in DW as measured by DLS. DLS: Dynamic light scattering; DW: Distilled water; NP: Nanoparticle; TEM: Transmission electron microscopy; XRD: X-ray diffraction.

Table 3. Physicochemical characterization of ZnO and TiO₂ nanoparticles.

Particle material	Crystallinity	Composition [†]	Primary size (nm) [‡]	Hydrodynamic size (nm) [§]	Surface area (m ² /g)	Zeta potential (mV)	Endotoxin (ng/ml)
ZnO	Hexagonal (zinc oxide > 97%)	72% Zn, 26% O, 2% C	50	450.6	32.17	32.9	N.D.
TiO ₂	Spherical (anatase > 99.7%)	60% Ti, 40% O	25	209.5	96.32	10.8	N.D.

[†]NPs were measured by EDS.[‡]NP primary sizes were measured by TEM.[§]NPs were dispersed in DW and measured by a DLS method.

DLS: Dynamic light scattering; EDS: Energy dispersive spectroscopy; N.D.: Not detectable; NP: Nanoparticle; TEM: Transmission electron microscopy.

nation was found. The physicochemical properties of the ZnO and TiO₂ NPs are summarized in Table 3.

Biodistribution of ZnO & TiO₂ NPs

Compared with the control group, in the ZnO NPs and TiO₂ NPs groups, there was no significant increase in the Zn concentration (Figure 3B) or Ti concentration (Figure 3D) in blood and tissues, respectively; however, the Zn concentration significantly increased in both the taste nerves and in the brain tissues in the ZnO NPs group (Figure 3A). The same pattern was observed for the Ti concentration in the TiO₂ NPs group (Figure 3C). This result indicated that the NPs were taken up by the taste buds, transported along the taste nerve, translocated to the brain and deposited, suggesting that the tongue-instilled NPs were mainly transported into the taste nerve, not the blood or tissues.

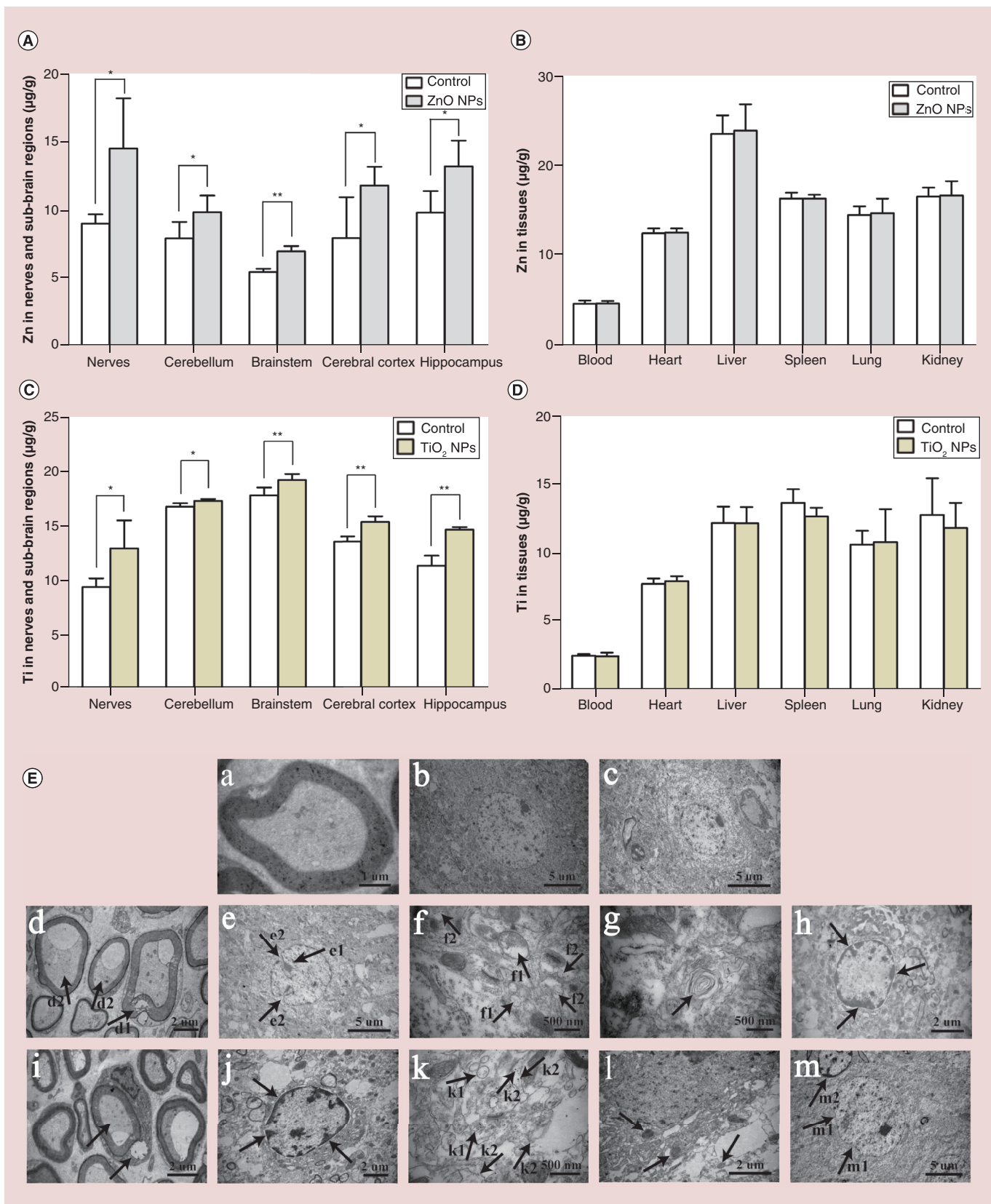
Accumulation in the brain & ultrastructural changes

Assessing where NPs are located and accumulate in the brain is an important first step. The ultrastructural changes in the nerve tissue (CT) and neurons of the brains in the rats are presented in Figure 3E. TEM analysis revealed that the ZnO NPs and TiO₂ NPs mainly accumulated in neural synapses. In the control group, the morphological structures of the myelin sheath and the lamellar structure in the nerve tissue were

intact (Figure 3E-a); moreover, the neurons contained an elliptical nucleus with homogeneous chromatin, organelles with regular shapes and intact membranes in the cerebral cortex (Figure 3E-b) and hippocampus (Figure 3E-c). Compared with that in the control group, the ultrastructure of the nerves (CT) and neurons in the ZnO NPs group presented a vacuolate myelin sheath, damaged lamellar structure and atrophied axoplasm (Figure 3E-d). The nuclei sagged in the neurons, which featured an irregular cell membrane (Figure 3E-e), prominent mitochondrial swelling and cristae fragmentation, and ZnO NPs were scattered around the neural synapses (Figure 3E-f), with the appearance of autophagosomes in the cerebral cortex (Figure 3E-g). Karyopyknosis and karyorrhexis were also observed in glial cells in the hippocampus (Figure 3E-h). The ultrastructure of the nerve and neuron from rats in the TiO₂ NPs group presented axoplasm atrophied in a myelin sheath wrapped by Schwann cells, vacuoles in the cytoplasm (Figure 3E-i), karyopyknosis and karyorrhexis in the glial cells (Figure 3E-j), prominent mitochondrial swelling, cristae fragmentation, TiO₂ NPs scattered around the neural synapses (Figure 3E-k) and many lysosomes (Figure 3E-l). In addition, the nuclei sagged in the neurons, which featured an irregular cell membrane, and karyopyknosis and karyorrhexis were observed in the glial cells in the hippocampus (Figure 3E-m). These results confirmed that ZnO NPs and TiO₂ NPs translocated into the brain and that

Figure 3. Concentrations of Zn and Ti in tissues and ultrastructure of nerve and brain tissues. The concentrations of Zn in the nerves (CT and glossopharyngeal nerve) and brain (A), tissues (B) and Ti in the nerves (CT and glossopharyngeal nerve) and brain (C) and tissues (D) were evaluated using ICP-MS. (E) Ultrastructure of nerve and brain tissues by TEM. (a-c) Control group: (a) nerve tissue (CT), (b) cerebral cortex and (c) hippocampus. (d-h) ZnO NPs group: (d) nerve tissue (CT), d1: vacuolate myelin sheath, damaged lamellar structure, d2: atrophied axoplasm (e-g) cerebral cortex, e1: nuclei sagged, e2 irregular cell membrane, f1: mitochondrial swelling and cristae fragmentation, f2: ZnO NPs scattered around the neural synapses, g: autophagosomes, (h) hippocampus: karyopyknosis and karyorrhexis. (i-m) TiO₂ NPs group: (i) nerve tissue (CT): axoplasm atrophied, (j-l) cerebral cortex, j: karyopyknosis and karyorrhexis, k1: mitochondrial swelling and cristae fragmentation, k2: TiO₂ NPs scattered around the neural synapses, l: lysosomes, (m) hippocampus, m1: irregular cell membrane, m2: karyopyknosis and karyorrhexis. Related changes are identified by the black arrows in the figures. Values are the mean \pm S.D. n = 4 for nerves in each group, n = 6 for the brain tissues in each group. Significance versus vehicle control: *p < 0.05, **p < 0.01.

CT: Chorda tympani; ICP-MS: Inductively coupled plasma mass spectrometry; NP: Nanoparticle; S.D.: Standard deviation; TEM: Transmission electron microscopy.



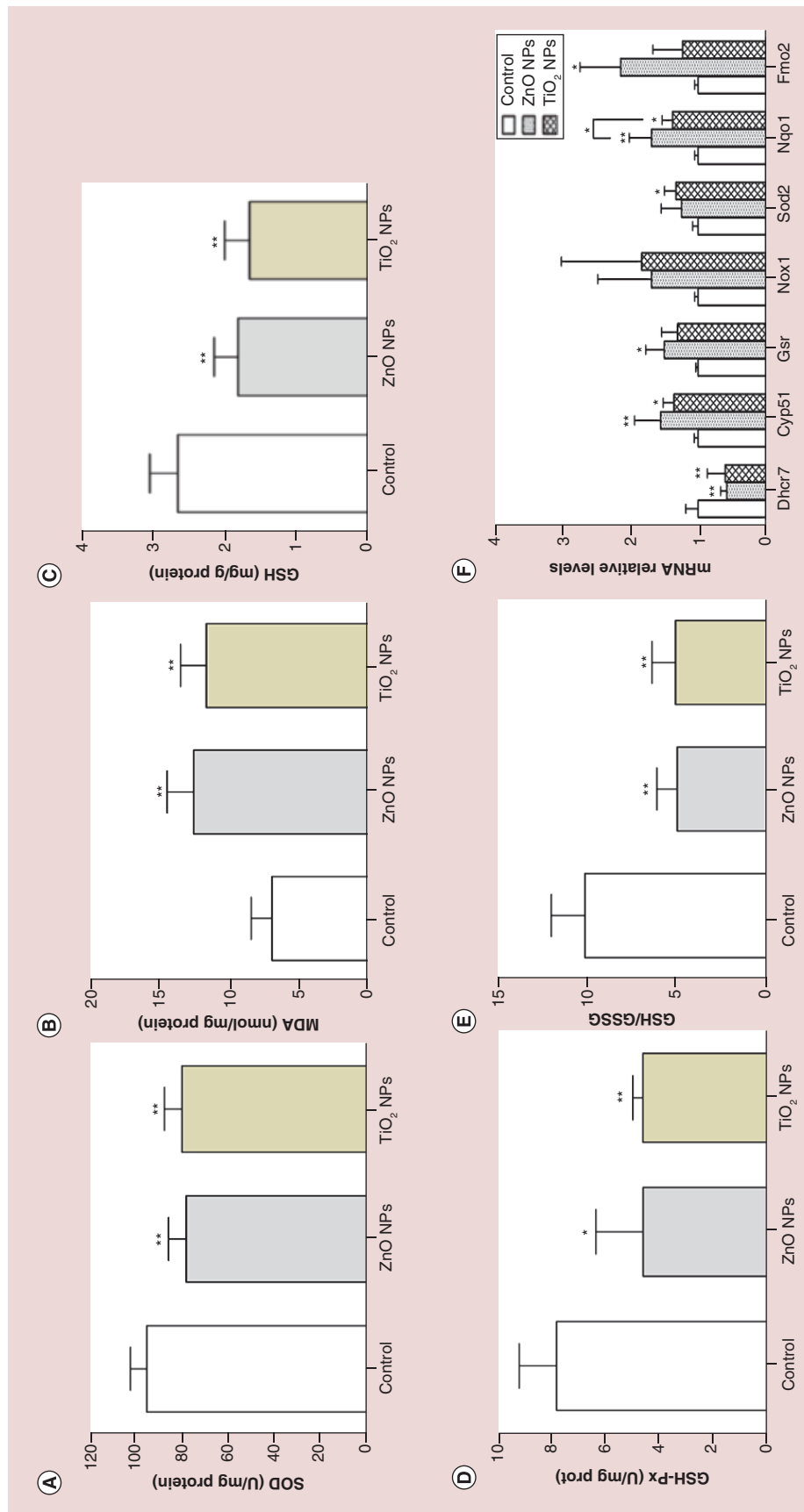
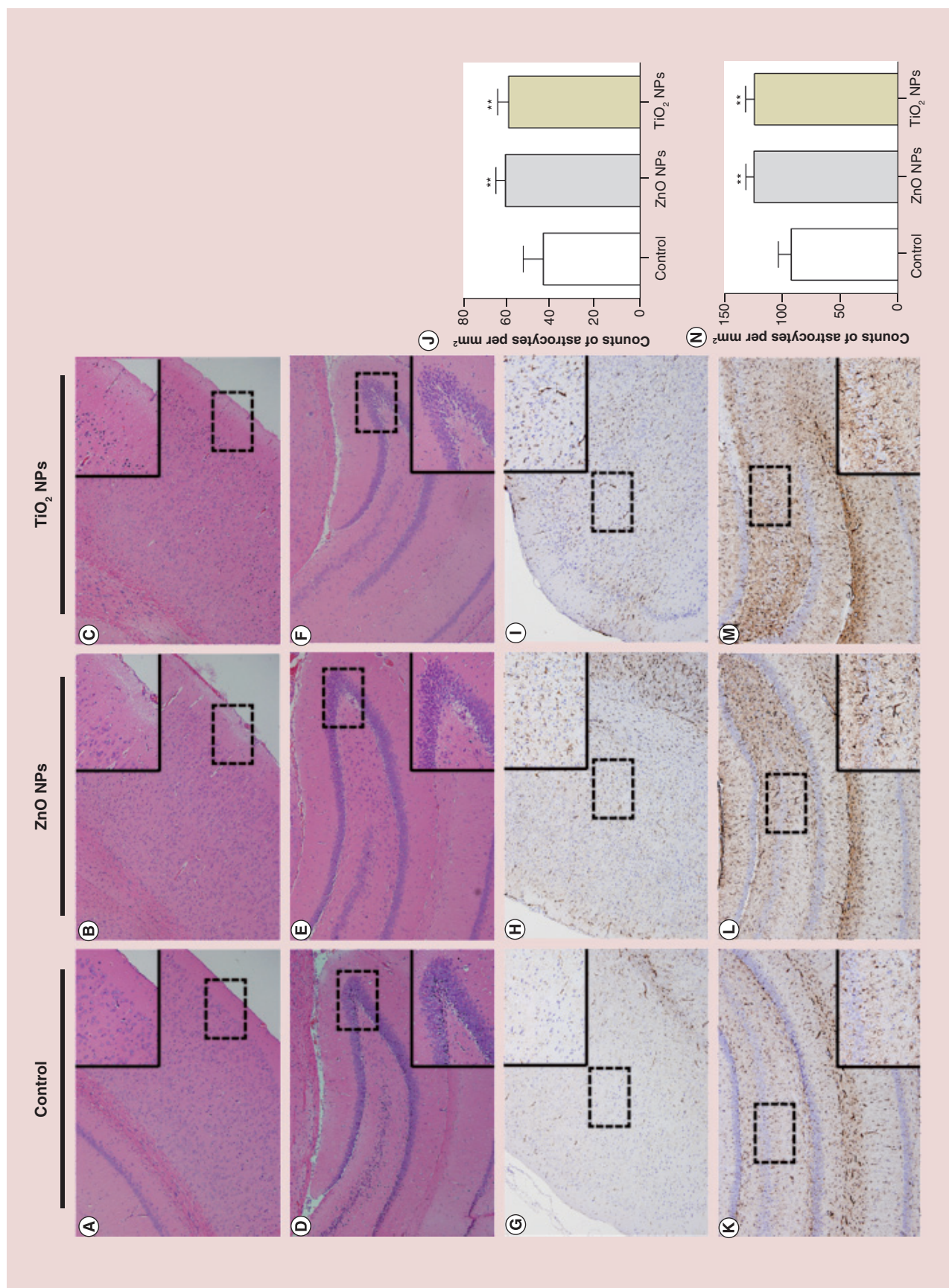


Figure 4. The status of oxidative stress and expression of oxidative stress-related genes in rats. The data are presented as means \pm S.D., $n = 6$. Significance versus control group: * $p < 0.05$, ** $p < 0.01$. S.D.: Standard deviation.

Figure 5. Histopathological and immunohistochemical evaluation of brain tissues in rats (see facing page). Six rats in each group were used for histological examination ($n = 6$). Sections of brain tissues were stained with HE (A-F) and GFAP (G-I). Images (A-C, G-I) and (D-F, K-M) show the architecture of the cerebral cortex (gustatory cortex) and hippocampus, respectively. The top or bottom right corner (400 \times) are enlarged images of (A-I, K-M; 100 \times). The brain tissues of the rats treated with ZnO NPs and TiO₂ NPs exhibited slight abnormalities in brain structure, with more sparse tissue in the cerebral cortex and hippocampus (A-F). Cell counting analysis of GFAP-positive astrocytes in the cerebral cortex and hippocampus (J and N, number/mm²).



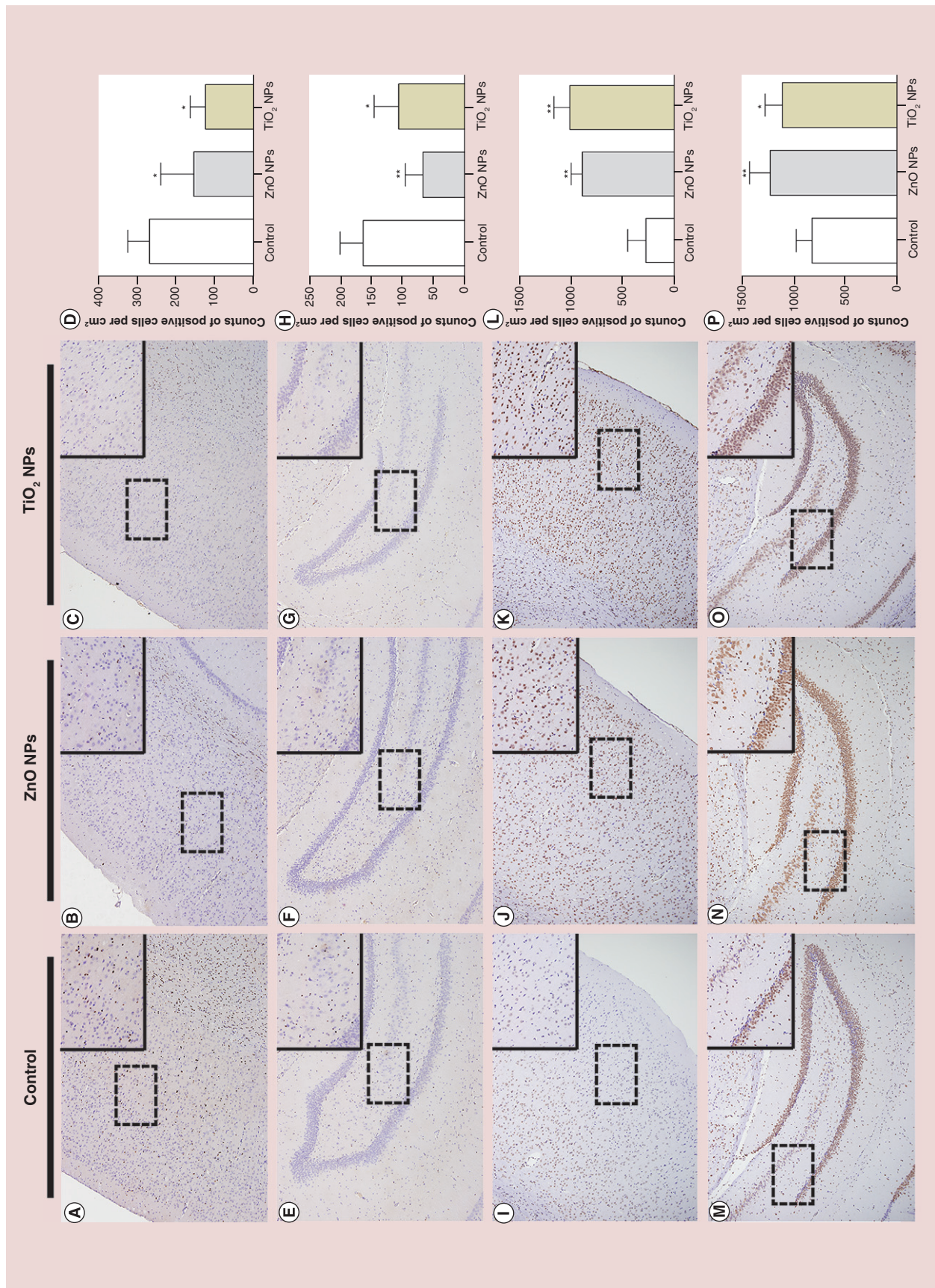


Figure 6. Immunohistochemical staining in the cerebral cortex (gustatory cortex) and hippocampus of rats. Histological examination was performed in six rats from each group (n = 6). Sections of brain tissues were stained with Ki-67 (A–C, E–G) and 8-OHdG (I–K, M–O). The top right corner (400 \times) of each image shows an enlarged image in (A–C, E–G, I–K, M–O; 100 \times). Cell counting analysis of Ki-67- and 8-OHdG-positive cells in the cerebral cortex and hippocampus (D, H, L & P, number/cm²). 8-OHdG: 8-Hydroxy-2-deoxyguanosine.

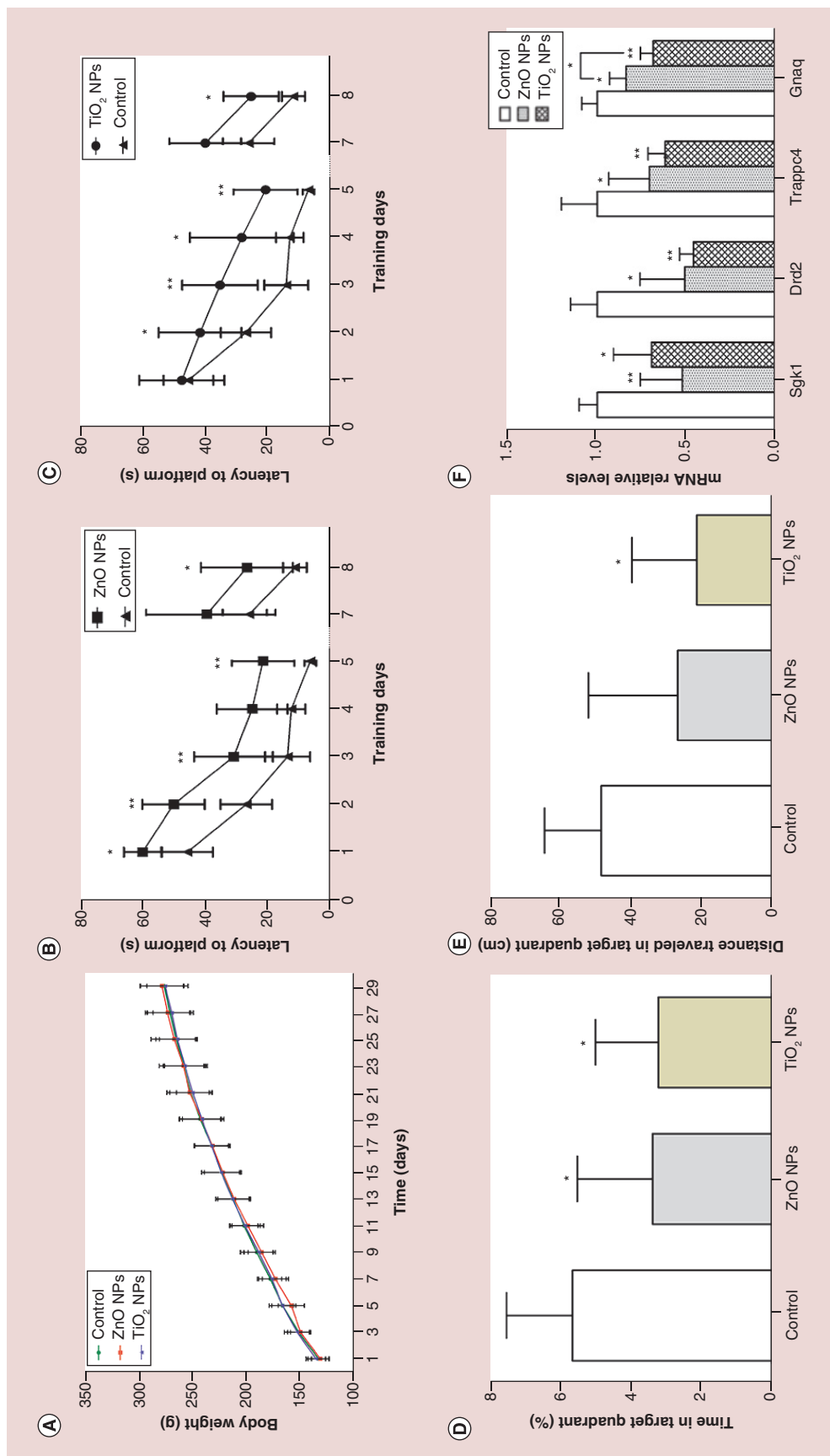


Figure 7. Performance of rats in the Morris water maze test. (A) Body weight gain in rats exposed to ZnO NPs and TiO₂ NPs. No significant difference was observed compared with the control group. (B) Rats exposed to ZnO NPs and the control group received training on days 1–5, 7 and 8. (C) Rats exposed to TiO₂ NPs and the control group received training on days 1–5, 7, 8. (D) The percentage of time spent in the target quadrant of the former platform position on day 6. (E) Distance travelled in the target quadrant on day 6. (F) Expression of learning- and memory-related genes in rats. Data are expressed as means \pm S.D., $n = 6$ for each group. Significance versus control group: * $p < 0.05$, ** $p < 0.01$. NP: Nanoparticle; S.D.: Standard deviation.

the structure of the nerves and the morphology of the organelles in brain tissue had been damaged, which may impair learning and memory ability in rats.

Oxidative damage in the brain

The levels of superoxide dismutase (SOD, Figure 4A), malondialdehyde (MDA, Figure 4B), glutathione (GSH, Figure 4C), glutathione-peroxidase (GSH-Px, Figure 4D) and glutathione/oxidized glutathione (GSH/GSSG, Figure 4E) in rats were determined in this study. Compared with the levels in the control group, the levels of SOD, GSH, GSH-Px and GSH/GSSG were significantly decreased in rats exposed to ZnO NPs and TiO₂ NPs, whereas the levels of MDA were significantly increased in the brain. No significant difference was observed between rats exposed to ZnO NPs and those exposed to TiO₂ NPs. These results indicated that the rats' exposure to ZnO NPs and TiO₂ NPs caused an imbalance of oxidative stress in the brain, which may induce brain damage. The results of qRT-PCR analysis of genes associated with oxidative stress were consistent with the results of the biochemical assays. Compared with their expression in the control group, significantly upregulated Cyp51, Gsr, Nqo1 and Fmo2 expression and downregulated Dhcr7 expression were observed in ZnO-NP-treated rats, whereas significantly upregulated Cyp51, Sod2 and Nqo1 expression and downregulated Dhcr7 expression were observed in TiO₂-NP-treated rats (Figure 4F). Moreover, Nqo1 was more highly upregulated in the ZnO NPs group than in the TiO₂ NPs group. The expression of other genes did not differ significantly between the ZnO NPs group and the TiO₂ NPs group. These data demonstrated that the expression of oxidative stress-related genes was significantly changed in the NPs-exposure groups, further demonstrating that the oxidative stress defence system was damaged by NPs exposure.

Histopathological changes in brain tissues

We examined the pathological histology of the brain in rats using hematoxylin-eosin staining. Representative micrographs of the brain sections (cerebral cortex and hippocampus) are shown in Figure 5A–F. The brain tissues of the rats exposed to either ZnO NPs or TiO₂ NPs showed slight injuries in the brain structure with more sparse tissue. These changes did not appear in the control group. There were no obvious pathological changes in the rats. These results indicate that NPs entering the brain tissue cause minor damage to the cerebral cortex and hippocampus.

Immunohistochemical changes in brain tissues

To further evaluate neurotoxicity, immunohistochemi-

cal analysis was conducted. We performed GFAP (Figure 5G–I & K–M), Ki-67 (Figure 6A–C & E–G) and 8-OHdG (Figure 7I–K & M–O) immunohistochemistry to examine the number of astrocytes in the brain and the effects of the ZnO NPs and TiO₂ NPs on proliferation and DNA damage in brain cells. Following the administration of ZnO NPs and TiO₂ NPs, the number of astrocytes (brown) significantly increased in the cerebral cortex and hippocampus compared with the number in the control group (Figure 5J & N). In addition, the number of Ki-67 positively stained (brown) cells in the cerebral cortex and hippocampus significantly decreased (Figure 6D & H). Moreover, the nuclei of brain cells positively stained by 8-OHdG (Figure 6L & P) significantly increased. These analyses demonstrate that the NPs that translocated into brain tissues suppressed cell proliferation, caused DNA damage and increased astrocytes.

The effect of ZnO & TiO₂ NPs on spatial learning & memory

During the experiment, the rats were weighted every other day between days 1 and 29 and sacrificed at 24-h postexposure (on day 30). Compared with the control group, the ZnO NP and TiO₂ NP groups exhibited no significant differences in BW. These data suggest that instillation of NPs through the tongue had no detectable influence on rat growth and development. The BW changes over 30 days are shown in Figure 7A.

The spatial cognition capability of rats was measured using the MWM test. Interestingly, the results in Figure 6 showed that for all animals, the latency of the rats reaching the platform decreased in the acquisition phase. Moreover, compared with the control group, the rats exposed to ZnO NPs on training days 1, 2, 3 and 5 presented significantly longer escape latency when finding the platform (Figure 6B), while rats exposed to TiO₂ NPs on training days 2, 3, 4 and 5 presented significant longer escape latency when finding the platform (Figure 7C). During the first day of reacquisition training (day 7), rats in the ZnO NPs and TiO₂ NPs groups presented no differences from the control rats but presented significant longer escape latency on the second day (day 8). During the probe test (day 6), rats in the ZnO NPs and TiO₂ NPs groups remained in the target quadrant for a shorter time (Figure 7D). Furthermore, rats in the TiO₂ NPs group travelled less distance in the target quadrant than the control group, while the ZnO NPs group showed no significant difference (Figure 7E).

To further verify the effect on learning and memory, the related genes were evaluated using qRT-PCR. All four genes, *Sgk1*, *Drd2*, *Trappc4* and *Gnaq*, were significantly downregulated in the ZnO NP and TiO₂

NP groups compared with their expression in the control group (**Figure 6F**). Moreover, the decrease in *Gnaq* was significantly greater in the TiO₂ NPs group than in the ZnO NPs group. These analyzes suggest that the learning and memory ability of rats may be attenuated by NPs.

Discussion

As demonstrated in our previous review, ZnO and TiO₂ in nanoparticulate form are considered more highly absorbable than micron-sized particles through intraperitoneal injection, intravenous injection and oral administration, among other methods. This absorption is due to their peculiar physicochemical properties, such as their size, shape, charge and surface modifications, which have an important influence on their interactions with cells [39]. NPs are taken up by cells through endocytosis, endocytosis and phagocytosis, then transported to CNS via axons [40,41]. NPs with smaller size [42] and larger surface area are more likely to induce cell damage, lead to apoptosis [43]. The positively charged NPs are more likely to accumulate in the cells than negatively charged or uncharged particles [44]. Probably because NPs with smaller size larger, surface area and positively charged can be more easily taken up by cells through endocytosis, endocytosis and phagocytosis. The physicochemical properties of ZnO NPs and TiO₂ NPs are illustrated in **Table 3 & Figure 2**. ZnO NPs and TiO₂ NPs used in this study have small particle size, large specific surface area, positive charge, homogeneous suspension, more easily taken up by cells and cause neurotoxic effect. The interaction mechanisms of NPs with biological systems are different from those of bulk chemicals [45,46], and ZnO NPs have been reported to produce higher toxicity than their bulk counterparts [47]. In recent years, it has been found that NPs not only pass through the BBB [48,49] and placental barrier [50–52] but are also transported along the nerve and deposited in the brain. The most well-known neural transport pathway is the olfactory nerve pathway [11,12]. NPs can translocate in the CNS (hippocampus and striatum) through the olfactory nerve pathway after inhalation or intranasal instillation exposure. In addition to the olfactory nerve pathway such as inhalation or intranasal instillation exposure, the pathway of taste nerve translocation is also an important pathway that cannot be ignored. However, there has been no report on whether NPs can be translocated into the brain via the taste nerve. Therefore, this study was conducted to investigate whether the NPs can translocate into the brain via the taste nerve and to assess their central neurotoxicity.

To determine if NPs are translocated into the brain only through the taste nerve pathway rather than the

BBB, in the study, the NPs suspension was carefully instilled only on the tongue and was not allowed to flow into the esophagus. The tongue was then rinsed with DW repeatedly until no suspension residue remained after administration. It has been reported that the oral administration of ZnO NPs increases the zinc concentration in the plasma over 24 h and that the NPs are distributed to the organs within 72 h [53]. After oral administration, ZnO NPs and TiO₂ NPs are taken up by the GI tract and accumulate in tissues such as the liver, kidney, lung and spleen, leading to toxic effects [37,53–56]. However, in our study, there was no significant Zn or Ti accumulation in blood and other tissues, indicating that ZnO NPs and TiO₂ NPs are transported to the brain via the taste nerve, which does not directly enter the blood (**Figure 3B & D**).

Due to the special complex network of sensory nerve endings between the nose and olfactory bulb, the inhaled/instilled NPs can first transport directly across the nasal mucosa via the olfactory nerve tract, enter into the olfactory bulb, thereby circumventing the BBB and finally deposit in brain such as olfactory bulb, hippocampus, cerebral cortex, cerebellum and striatum [57–59]. Considering the similarity of olfactory and taste nerves, our current study suggests that after tongue instillation with ZnO NPs and TiO₂ NPs for 30 days, NPs were first taken up by the cells in the taste buds and entered the afferent taste fibers. The NPs were then transported along the CT, where NPs were taken up by the anterior two thirds of the taste buds, or the glossopharyngeal nerve, where NPs were taken up by the posterior third of the taste buds, and then transferred to the NST, parabrachial nucleus, posterior thalamic nucleus (**Figure 1**), ultimately accumulating in brain such as the cerebellum, brainstem, cerebral cortex and hippocampus after exposure to tongue instillation (**Figure 3A & C**).

The results were further confirmed by TEM analysis (**Figure 3E**). The TEM observations clearly showed that the NPs translocated into the neural synapses in the cerebral cortex (**Figure 3E-f & E-k**), activating autophagosomes and lysosomes (**Figure 3E-g & I**). Similar to our study, large amounts of NPs have been shown previously to induce autophagy [60,61] and increase lysosomes [62]. Autophagy is a cellular process for degrading protein aggregates and damaged organelles such as mitochondria [63,64] and plays a central role in neurodegeneration [65] as well as lysosomal dysfunction [66].

We demonstrated that exposure to ZnO NPs and TiO₂ NPs induces oxidative stress in the CNS. Similar to transport along the olfactory nerve, NPs transport along the taste nerve and significantly deposit in the brain (**Figure 4A–E**). It has been demonstrated that exposure to metal oxide NPs increases brain oxidative

stress and induces potential neurotoxicity [67–69]. In this study, significantly decreased SOD, GSH, GSH-Px, GSH/GSSG concentrations and an increased MDA concentration were identified in the brain homogenate of ZnO-NPs-treated and TiO₂-NPs-treated rats. When genes related to oxidative stress were further evaluated by qRT-PCR, significantly upregulated Cyp51, Gsr, Nqo1, Fmo2 expression and downregulated Dhcr7 expression were identified in ZnO-NPs-treated rats, while significantly upregulated Cyp51, Sod2, Nqo1 expression and downregulated Dhcr7 expression were identified in TiO₂-NPs-treated rats (Figure 4F).

The central neurotoxicity was identified in rats after tongue instillation of ZnO NPs and TiO₂ NPs. It has been well demonstrated that oxidative stress plays a critical role in the common mechanism of NP toxicity [70]. Abundant evidence indicates that ZnO NPs and TiO₂ NPs that accumulate in the brain can cause pathological changes, cell damage and apoptosis and ultimately lead to neurodegeneration through reactive oxygen species production and oxidative stress induction [71–73]. The histopathology examination showed that tongue-instilled ZnO NPs and TiO₂ NPs might cause slight injury to the cerebral cortex and hippocampus (Figure 5A–F). In addition, there was a significant increase in the expression of GFAP in the cerebral cortex and hippocampus (Figure 4J & N). GFAP is an intermediate filament and acts as a specific cellular marker for activated astrocytes with increased expression. Astroglial activation and increased GFAP expression in the CNS can directly inhibit the regrowth and regeneration of axons [74], resulting in neurodegeneration [75–77]. Moreover, significantly reduced proliferation of brain cells (Figure 5D & H) and DNA damage (Figure 5L & P) were observed by immunohistochemical analysis. There was no significant difference between ZnO NPs and TiO₂ NPs in immunohistochemical analysis.

The CNS is potentially vulnerable to attacks by ZnO NPs and TiO₂ NPs, and hippocampal cells are susceptible to oxidative stress [78]. Substantial evidence suggests the hippocampus is closely related to cognitive ability, including learning and memory. Thus, the effects of ZnO NPs and TiO₂ NPs exposure on neurocognitive function in rats were explored. Compared with the control group, rats in the ZnO NP and TiO₂ NP groups showed complex behavior deficits in the MWM, and their navigational strategies were affected. The deficits prevented the rats from searching for the platform efficiently (Figure 7B–E). These findings strongly suggest that exposure to ZnO NPs and TiO₂ NPs causes neurodegeneration. The impairment of learning and memory is mainly due to the oxidative stress [71,79]. Evidence suggests that rats exposed to

ZnO NPs lack flexibility in their learning and memory and that their spatial learning and memory ability may be impaired by changes in their synaptic plasticity [7]. Interestingly, a single intravenous injection of ZnO NPs does not affect rat behavior after 14 days [80], probably because the rats are exposed to NPs only for a short time and the early NPs that entered the body were excreted. Similarly, TiO₂ NPs in the brain can also lead to neurodegeneration [81]. Evidence suggests that TiO₂ NPs can pass through the placental barrier and impair the developing fetus [82,83]. Additionally, the behavioral performance results were further confirmed by qRT-PCR. In this study, significantly downregulated Sgk1, Drd2, Trappc4 and Gnaq expression was identified in ZnO-NPs-treated and TiO₂-NPs-treated rats (Figure 7F). Sgk participates in axonal regeneration after brain injury and improves spatial learning and memory ability in rats [84,85]. Drd2 is a dopamine D2 receptor, which is closely related to the regulation of learning and memory in hippocampus [86]. Trappc4, also known as Sbdn, has a positive relationship with learning and memory by activating the ERK pathway to promote vesicle trafficking and stimulating long-term potentiation in hippocampal and cortical [86,87]. Gnaq is a guanine nucleotide-binding protein member that is expressed ubiquitously in the CNS and is positively related to learning and memory [88]. Interestingly, mice with Gαq knockout demonstrated affected motor coordination and strength [89]. The downregulated Gnaq expression in the TiO₂ NPs group was significantly lower than in the ZnO NPs group suggesting that rats exposed to TiO₂ NPs demonstrate a worse performance in motor coordination and strength than those exposed to ZnO NPs.

Conclusion

Our results demonstrate that ZnO NPs and TiO₂ NPs can be taken up by taste buds and translocated into the brain via the taste nerves (CT and glossopharyngeal nerves) after tongue instillation for 30 days. We observed a high content of ZnO NPs and TiO₂ NPs deposited in the brain. Furthermore, the deposited NPs in the brain may induce an oxidative stress imbalance, inhibiting cell proliferation, causing DNA damage and resulting in neurodegeneration. Rats exposed to ZnO NPs and TiO₂ NPs showed significant deficits in behavioral performance. There is no significant difference between ZnO NP and TiO₂ NP in neurotoxicity by tongue instillation. In general, this study investigates a new pathway for NPs to translocate into the brain and evaluates their central neurotoxicity. Further investigation regarding the influence of NPs on the taste nerve pathway and neurodegeneration is necessary.

Acknowledgements

The authors would like to thank Jiang Danyu and the State Key Laboratory of High Performance Ceramics and Superfine Microstructure for NP characterizations of this study.

Financial & competing interests disclosure

This work was supported by the Natural Science Foundation of Guang-dong Province of China (2016A030313673 and 2015A030313299), the Zhejiang Provincial Natural Science Foundation of China (LY16H140003), the Wenzhou Municipal Science and Technology Bureau Foundation of China (Y20150070) and Military Medical Science and Technology Project (14QNP077). The authors have no other relevant affili-

ations or financial involvement with any organization or entity with a financial interest in or financial conflict with the subject matter or materials discussed in the manuscript apart from those disclosed.

No writing assistance was utilized in the production of this manuscript.

Ethical conduct of research

All animal experiments were performed in compliance with the regulations and guidelines of the National Ethics Committee on Animal Welfare of China. The approval number provided by the Southern Medical University ethical committee was 2015–021.

Summary points

- ZnO nanoparticles (NPs) and TiO₂ NPs have been widely used in numerous fields. The increasing applications of NPs present potential health risks.
- At present, study found that NPs can be transported along nerves. However, there are no published reports on whether NPs can be transported into the CNS via the taste nerve pathway.
- High content of ZnO NPs and TiO₂ NPs deposited in the nerves and brain after tongue instillation with ZnO NPs and TiO₂ NPs suspension, respectively, every other day for 30 days.
- Transmission electron microscopy observation showed morphological changes of neurons and organelles. Moreover, ZnO NPs and TiO₂ NPs obvious accumulate in the synapses.
- Exposure to ZnO NPs and TiO₂ NPs caused an imbalance of oxidative stress in the brain, and the expression of oxidative stress-related genes had consistent changes.
- Histopathological changes such as decreased proliferation, increased DNA damage and astrocytes were observed in the cerebral cortex and hippocampus of rats.
- Exposure to ZnO NPs and TiO₂ NPs impaired the learning and memory ability of rats in the Morris water maze test, and the expression of learning- and memory-related genes had consistent changes.
- ZnO NPs and TiO₂ NPs can be taken up by taste buds, then translocated to the medulla nucleus of the solitary tract, parabrachial nucleus, thalamic nucleus, ultimately accumulating in the gustatory cortex after exposure to tongue instillation.

References

Papers of special note have been highlighted as: • of interest;
•• of considerable interest

- 1 Bleeker EA, De Jong WH, Geertsma RE *et al.* Considerations on the EU definition of a nanomaterial: science to support policy making. *Regul. Toxicol. Pharmacol.* 65(1), 119–125 (2013).
- 2 Horie M, Stowe M, Tabei M, Kuroda E. Pharyngeal aspiration of metal oxide nanoparticles showed potential of allergy aggravation effect to inhaled ovalbumin. *Inhal. Toxicol.* 27(3), 181–190 (2015).
- 3 Konduru NV, Murdaugh KM, Sotiriou GA *et al.* Bioavailability, distribution and clearance of tracheally-instilled and gavaged uncoated or silica-coated zinc oxide nanoparticles. *Part. Fibre Toxicol.* 11, 44 (2014).
- 4 Geraets L, Oomen AG, Krystek P *et al.* Tissue distribution and elimination after oral and intravenous administration of different titanium dioxide nanoparticles in rats. *Part. Fibre Toxicol.* 11, 30 (2014).
- 5 Ilves M, Palomaki J, Vippola M *et al.* Topically applied ZnO nanoparticles suppress allergen induced skin inflammation but induce vigorous IgE production in the atopic dermatitis mouse model. *Part. Fibre Toxicol.* 11, 38 (2014).
- 6 Medina C, Santos-Martinez MJ, Radomski A, Corrigan OI, Radomski MW. Nanoparticles: pharmacological and toxicological significance. *Br. J. Pharmacol.* 150(5), 552–558 (2007).
- 7 Han D, Tian Y, Zhang T, Ren G, Yang Z. Nano-zinc oxide damages spatial cognition capability via over-enhanced long-term potentiation in hippocampus of Wistar rats. *Int. J. Nanomedicine* 6, 1453–1461 (2011).
- 8 Hu R, Zheng L, Zhang T *et al.* Molecular mechanism of hippocampal apoptosis of mice following exposure to titanium dioxide nanoparticles. *J. Hazard. Mater.* 191(1–3), 32–40 (2011).
- 9 Jiang X, Rocker C, Hafner M, Brandholt S, Dorlich RM, Nienhaus GU. Endo- and exocytosis of zwitterionic quantum dot nanoparticles by live HeLa cells. *ACS Nano* 4(11), 6787–6797 (2010).
- 10 Kao YY, Cheng TJ, Yang DM, Wang CT, Chiung YM, Liu PS. Demonstration of an olfactory bulb-brain translocation pathway for ZnO nanoparticles in rodent cells *in vitro* and *in vivo*. *J. Mol. Neurosci.* 48(2), 464–471 (2012).
- 11 Kreyling WG. Discovery of unique and ENM-specific pathophysiologic pathways: comparison of the translocation of inhaled iridium nanoparticles from nasal epithelium

- versus alveolar epithelium towards the brain of rats. *Toxicol. Appl. Pharmacol.* 299, 41–46 (2016).
- 12 Kanazawa T, Akiyama F, Kakizaki S, Takashima Y, Seta Y. Delivery of siRNA to the brain using a combination of nose-to-brain delivery and cell-penetrating peptide-modified nano-micelles. *Biomaterials* 34(36), 9220–9226 (2013).
- 13 Dao AQ, Zheng B, Liu H et al. Facile synthesis of r-GO@Pd/TiO₂ nanocomposites and its photocatalytic activity under visible light. *J. Nanosci. Nanotechnol.* 16(4), 3557–3563 (2016).
- 14 Fazli Y, Shariatinia Z, Kohsari I, Azadmehr A, Pourmortazavi SM. A novel chitosan-polyethylene oxide nanofibrous mat designed for controlled co-release of hydrocortisone and imipenem/cilastatin drugs. *Int. J. Pharm.* 513(1–2), 636–647 (2016).
- 15 Zhao CY, Tan SX, Xiao XY, Qiu XS, Pan JQ, Tang ZX. Effects of dietary zinc oxide nanoparticles on growth performance and antioxidative status in broilers. *Biol. Trace Elem. Res.* 160(3), 361–367 (2014).
- 16 Weir A, Westerhoff P, Fabricius L, Hristovski K, Von Goetz N. Titanium dioxide nanoparticles in food and personal care products. *Environ. Sci. Technol.* 46(4), 2242–2250 (2012).
- 17 Lomer MC, Thompson RP, Commissio J, Keen CL, Powell JJ. Determination of titanium dioxide in foods using inductively coupled plasma optical emission spectrometry. *Analyst* 125(12), 2339–2343 (2000).
- 18 Small DM. Flavor is in the brain. *Physiol. Behav.* 107(4), 540–552 (2012).
- 19 Rolls ET. Taste, olfactory and food texture reward processing in the brain and the control of appetite. *Proc. Nutr. Soc.* 71(4), 488–501 (2012).
- 20 Veldhuizen MG, Shepard TG, Wang MF, Marks LE. Coactivation of gustatory and olfactory signals in flavor perception. *Chem. Senses* 35(2), 121–133 (2010).
- 21 Chaudhari N, Roper SD. The cell biology of taste. *J. Cell Biol.* 190(3), 285–296 (2010).
- 22 Doty RL. Gustation. *Wiley Interdiscip. Rev. Cogn. Sci.* 3(1), 29–46 (2012).
- 23 Lindemann B. Receptors and transduction in taste. *Nature* 413(6852), 219–225 (2001).
- 24 Roper SD. Signal transduction and information processing in mammalian taste buds. *Pflugers Arch.* 454(5), 759–776 (2007).
- 25 Doty RL, Heidt JM, Macgillivray MR et al. Influences of age, tongue region, and chorda tympani nerve sectioning on signal detection measures of lingual taste sensitivity. *Physiol. Behav.* 155, 202–207 (2016).
- 26 Stratford JM, Thompson JA, Finger TE. Immunocytochemical organization and sour taste activation in the rostral nucleus of the solitary tract of mice. *J. Comp. Neurol.* 525(2), 271–290 (2017).
- 27 Park SK, Lee DS, Bae JY, Bae YC. Central connectivity of the chorda tympani afferent terminals in the rat rostral nucleus of the solitary tract. *Brain Struct. Funct.* 221(2), 1125–1137 (2016).
- 28 Sun C, Hummeler E, Hill DL. Selective deletion of sodium salt taste during development leads to expanded terminal fields of gustatory nerves in the adult mouse nucleus of the solitary tract. *J. Neurosci.* 2016, 2913–2916 (2016).
- 29 Sammons JD, Weiss MS, Escanilla OD, Fooden AF, Victor JD, Di Lorenzo PM. Spontaneous changes in taste sensitivity of single units recorded over consecutive days in the brainstem of the awake rat. *PLoS ONE* 11(8), e0160143 (2016).
- 30 Sammons JD, Weiss MS, Victor JD, Di Lorenzo PM. Taste coding of complex naturalistic taste stimuli and traditional taste stimuli in the parabrachial pons of the awake, freely licking rat. *J. Neurophysiol.* 116(1), 171–182 (2016).
- 31 Kato T, Yamada Y, Yamamoto N. General visceral and gustatory connections of the posterior thalamic nucleus of goldfish. *J. Comp. Neurol.* 519(15), 3102–3123 (2011).
- 32 Schier LA, Blonde GD, Spector AC. Bilateral lesions in a specific subregion of posterior insular cortex impair conditioned taste aversion expression in rats. *J. Comp. Neurol.* 524(1), 54–73 (2016).
- 33 Avery JA, Gotts SJ, Kerr KL et al. Convergent gustatory and viscerosensory processing in the human dorsal mid-insula. *Hum. Brain Mapp.* 38(4), 2150–2164 (2017).
- 34 Zhang L, Bai R, Li B et al. Rutile TiO₂ particles exert size and surface coating dependent retention and lesions on the murine brain. *Toxicol. Lett.* 207(1), 73–81 (2011).
- 35 Gao L, Yang ST, Li S, Meng Y, Wang H, Lei H. Acute toxicity of zinc oxide nanoparticles to the rat olfactory system after intranasal instillation. *J. Appl. Toxicol.* 33(10), 1079–1088 (2013).
- 36 Grissa I, Guezguez S, Ezzi L et al. The effect of titanium dioxide nanoparticles on neuroinflammation response in rat brain. *Environ. Sci. Pollut. Res. Int.* 23(20), 20205–20213 (2016).
- 37 Cho WS, Kang BC, Lee JK, Jeong J, Che JH, Seok SH. Comparative absorption, distribution, and excretion of titanium dioxide and zinc oxide nanoparticles after repeated oral administration. *Part. Fibre Toxicol.* 10, 9 (2013).
- 38 Kim YR, Park JI, Lee EJ et al. Toxicity of 100 nm zinc oxide nanoparticles: a report of 90-day repeated oral administration in Sprague Dawley rats. *Int. J. Nanomedicine* 9(Suppl. 2), 109–126 (2014).
- 39 Feng X, Chen A, Zhang Y, Wang J, Shao L, Wei L. Central nervous system toxicity of metallic nanoparticles. *Int. J. Nanomedicine* 10, 4321–4340 (2015).
- 40 Simko M, Mattsson MO. Risks from accidental exposures to engineered nanoparticles and neurological health effects: a critical review. *Part. Fibre Toxicol.* 7, 42 (2010).
- 41 Asharani PV, Hande MP, Valiyaveetil S. Anti-proliferative activity of silver nanoparticles. *BMC Cell Biol.* 10, 65 (2009).
- 42 Kim TH, Kim M, Park HS, Shin US, Gong MS, Kim HW. Size-dependent cellular toxicity of silver nanoparticles. *J. Biomed. Mater. Res. A* 100(4), 1033–1043 (2012).
- 43 Xu Z, Liu C, Wei J, Sun J. Effects of four types of hydroxyapatite nanoparticles with different nanocrystal morphologies and sizes on apoptosis in rat osteoblasts. *J. Appl. Toxicol.* 32(6), 429–435 (2012).

- 44 Thorek DL, Tsourkas A. Size, charge and concentration dependent uptake of iron oxide particles by non-phagocytic cells. *Biomaterials* 29(26), 3583–3590 (2008).
- 45 Seok SH, Cho WS, Park JS *et al.* Rat pancreatitis produced by 13-week administration of zinc oxide nanoparticles: biopersistence of nanoparticles and possible solutions. *J. Appl. Toxicol.* 33(10), 1089–1096 (2013).
- 46 Oberdorster G, Oberdorster E, Oberdorster J. Nanotoxicology: an emerging discipline evolving from studies of ultrafine particles. *Environ. Health Perspect.* 113(7), 823–839 (2005).
- 47 Srivastav AK, Kumar M, Ansari NG *et al.* A comprehensive toxicity study of zinc oxide nanoparticles versus their bulk in Wistar rats: toxicity study of zinc oxide nanoparticles. *Hum. Exp. Toxicol.* 35(12), 1286–1304 (2016).
- 48 Yan H, Wang L, Wang J *et al.* Two-order targeted brain tumor imaging by using an optical/paramagnetic nanoprobe across the blood brain barrier. *ACS Nano* 6(1), 410–420 (2012).
- 49 Lai L, Zhao C, Su M *et al.* *In vivo* target bio-imaging of Alzheimer's disease by fluorescent zinc oxide nanoclusters. *Biomater. Sci.* 4(7), 1085–1091 (2016).
- 50 Osmond-Mcleod MJ, Oytam Y, Kirby JK, Gomez-Fernandez L, Baxter B, Mccall MJ. Dermal absorption and short-term biological impact in hairless mice from sunscreens containing zinc oxide nano- or larger particles. *Nanotoxicology* 8(Suppl. 1), 72–84 (2014).
- 51 Yamashita K, Yoshioka Y, Higashisaka K *et al.* Silica and titanium dioxide nanoparticles cause pregnancy complications in mice. *Nat. Nanotechnol.* 6(5), 321–328 (2011).
- 52 Cui Y, Chen X, Zhou Z *et al.* Prenatal exposure to nanoparticulate titanium dioxide enhances depressive-like behaviors in adult rats. *Chemosphere* 96, 99–104 (2014).
- 53 Baek M, Chung HE, Yu J *et al.* Pharmacokinetics, tissue distribution, and excretion of zinc oxide nanoparticles. *Int. J. Nanomedicine* 7, 3081–3097 (2012).
- Evaluates the biodistribution and excretion of ZnO nanoparticles (NPs; 20 and 70 nm) by oral administration.
- 54 Chen A, Feng X, Sun T, Zhang Y, An S, Shao L. Evaluation of the effect of time on the distribution of zinc oxide nanoparticles in tissues of rats and mice: a systematic review. *IET Nanobiotechnol.* 10(3), 97–106 (2016).
- 55 Wang J, Zhou G, Chen C *et al.* Acute toxicity and biodistribution of different sized titanium dioxide particles in mice after oral administration. *Toxicol. Lett.* 168(2), 176–185 (2007).
- 56 Wang Y, Chen Z, Ba T *et al.* Susceptibility of young and adult rats to the oral toxicity of titanium dioxide nanoparticles. *Small* 9(9–10), 1742–1752 (2013).
- Different ages may require different biomarkers for identifying and monitoring oral toxicity of NPs.
- 57 Zhang L, Bai R, Liu Y *et al.* The dose-dependent toxicological effects and potential perturbation on the neurotransmitter secretion in brain following intranasal instillation of copper nanoparticles. *Nanotoxicology* 6(5), 562–575 (2012).
- 58 Wang J, Liu Y, Jiao F *et al.* Time-dependent translocation and potential impairment on central nervous system by intranasally instilled TiO₂ nanoparticles. *Toxicology* 254(1–2), 82–90 (2008).
- Subtle differences in responses to anatase TiO₂ particles versus the rutile ones. Rutile ultrafine-TiO₂ particles are expected to have a little lower risk potential for producing adverse effects on CNS.
- 59 Bai R, Zhang L, Liu Y *et al.* Integrated analytical techniques with high sensitivity for studying brain translocation and potential impairment induced by intranasally instilled copper nanoparticles. *Toxicol. Lett.* 226(1), 70–80 (2014).
- 60 Stern ST, Adiseshaiah PP, Crist RM. Autophagy and lysosomal dysfunction as emerging mechanisms of nanomaterial toxicity. *Part. Fibre Toxicol.* 9, 20 (2012).
- 61 Peynshaert K, Manshian BB, Joris F *et al.* Exploiting intrinsic nanoparticle toxicity: the pros and cons of nanoparticle-induced autophagy in biomedical research. *Chem. Rev.* 114(15), 7581–7609 (2014).
- 62 Huang D, Zhou H, Gao J. Nanoparticles modulate autophagic effect in a dispersity-dependent manner. *Sci. Rep.* 5, 14361 (2015).
- 63 Mizushima N, Komatsu M. Autophagy: renovation of cells and tissues. *Cell* 147(4), 728–741 (2011).
- 64 Kim YM, Jung CH, Seo M *et al.* mTORC1 phosphorylates UVRAG to negatively regulate autophagosome and endosome maturation. *Mol. Cell* 57(2), 207–218 (2015).
- 65 Catalan-Figueroa J, Palma-Florez S, Alvarez G, Fritz HF, Jara MO, Morales JO. Nanomedicine and nanotoxicology: the pros and cons for neurodegeneration and brain cancer. *Nanomedicine (Lond.)* 11(2), 171–187 (2016).
- 66 Bourdenx M, Daniel J, Genin E *et al.* Nanoparticles restore lysosomal acidification defects: Implications for Parkinson and other lysosomal-related diseases. *Autophagy* 12(3), 472–483 (2016).
- 67 Shrivastava R, Raza S, Yadav A, Kushwaha P, Flora SJ. Effects of sub-acute exposure to TiO₂, ZnO and Al₂O₃ nanoparticles on oxidative stress and histological changes in mouse liver and brain. *Drug Chem. Toxicol.* 37(3), 336–347 (2014).
- 68 Zhao X, Ren X, Zhu R, Luo Z, Ren B. Zinc oxide nanoparticles induce oxidative DNA damage and ROS-triggered mitochondria-mediated apoptosis in zebrafish embryos. *Aquat. Toxicol.* 180, 56–70 (2016).
- 69 Ma L, Liu J, Li N *et al.* Oxidative stress in the brain of mice caused by translocated nanoparticulate TiO₂ delivered to the abdominal cavity. *Biomaterials* 31(1), 99–105 (2010).
- 70 Karmakar A, Zhang Q, Zhang Y. Neurotoxicity of nanoscale materials. *J. Food Drug Anal.* 22(1), 147–160 (2014).
- 71 Tian L, Lin B, Wu L *et al.* Neurotoxicity induced by zinc oxide nanoparticles: age-related differences and interaction. *Sci. Rep.* 5, 16117 (2015).
- 72 Czajka M, Sawicki K, Sikorska K, Popek S, Kruszewski M, Kapka-Skrzypczak L. Toxicity of titanium dioxide nanoparticles in central nervous system. *Toxicol. In vitro* 29(5), 1042–1052 (2015).

- 73 Wang J, Deng X, Zhang F, Chen D, Ding W. ZnO nanoparticle-induced oxidative stress triggers apoptosis by activating JNK signaling pathway in cultured primary astrocytes. *Nanoscale Res. Lett.* 9(1), 117 (2014).
- 74 Wilhelmsson U, Li L, Pekna M et al. Absence of glial fibrillary acidic protein and vimentin prevents hypertrophy of astrocytic processes and improves post-traumatic regeneration. *J. Neurosci.* 24(21), 5016–5021 (2004).
- 75 Wang J, Chen C, Liu Y et al. Potential neurological lesion after nasal instillation of TiO₂ nanoparticles in the anatase and rutile crystal phases. *Toxicol. Lett.* 183(1–3), 72–80 (2008).
- Nasal-instilled TiO₂ NPs could be translocated into the CNS and cause potential lesion of brain, and the hippocampus would be the main target within brain.
- 76 Liu Y, Gao Y, Liu Y, Li B, Chen C, Wu G. Oxidative stress and acute changes in murine brain tissues after nasal instillation of copper particles with different sizes. *J. Nanosci. Nanotechnol.* 14(6), 4534–4540 (2014).
- 77 Li XB, Zheng H, Zhang ZR et al. Glia activation induced by peripheral administration of aluminum oxide nanoparticles in rat brains. *Nanomedicine* 5(4), 473–479 (2009).
- 78 Yang Z, Liu ZW, Allaker RP et al. A review of nanoparticle functionality and toxicity on the central nervous system. *J. R. Soc. Interface* 7(Suppl. 4), S411–S422 (2010).
- 79 Heusinkveld HJ, Wahle T, Campbell A et al. Neurodegenerative and neurological disorders by small inhaled particles. *Neurotoxicology* 56 94–106 (2016).
- 80 Amara S, Ben-Slama I, Mrad I et al. Acute exposure to zinc oxide nanoparticles does not affect the cognitive capacity and neurotransmitters levels in adult rats. *Nanotoxicology* 8(Suppl. 1), 208–215 (2014).
- Acute intravenous injection of ZnO NPs does not affect neurotransmitter contents, locomotor activity and spatial working memory in adult rats.
- 81 Song B, Liu J, Feng X, Wei L, Shao L. A review on potential neurotoxicity of titanium dioxide nanoparticles. *Nanoscale Res. Lett.* 10(1), 1042 (2015).
- 82 Mohammadipour A, Fazel A, Haghiri H et al. Maternal exposure to titanium dioxide nanoparticles during pregnancy; impaired memory and decreased hippocampal cell proliferation in rat offspring. *Environ. Toxicol. Pharmacol.* 37(2), 617–625 (2014).
- Morris water maze test and the passive avoidance test showed that exposure to TiO₂ NPs significantly impaired learning and memory in offspring.
- 83 Mohammadipour A, Hosseini M, Fazel A et al. The effects of exposure to titanium dioxide nanoparticles during lactation period on learning and memory of rat offspring. *Toxicol. Ind. Health* 32(2), 221–228 (2016).
- 84 Imaizumi K, Tsuda M, Wanaka A, Tohyama M, Takagi T. Differential expression of *sgk* mRNA, a member of the Ser/Thr protein kinase gene family, in rat brain after CNS injury. *Brain Res. Mol. Brain Res.* 26(1–2), 189–196 (1994).
- 85 Tsai KJ, Chen SK, Ma YL, Hsu WL, Lee EH. *sgk*, a primary glucocorticoid-induced gene, facilitates memory consolidation of spatial learning in rats. *Proc. Natl Acad. Sci. USA* 99(6), 3990–3995 (2002).
- 86 Rocchetti J, Isingrini E, Dal Bo G et al. Presynaptic D2 dopamine receptors control long-term depression expression and memory processes in the temporal hippocampus. *Biol. Psychiatry* 77(6), 513–525 (2015).
- 87 Igaz LM, Winograd M, Cammarota M et al. Early activation of extracellular signal-regulated kinase signaling pathway in the hippocampus is required for short-term memory formation of a fear-motivated learning. *Cell. Mol. Neurobiol.* 26(4–6), 989–1002 (2006).
- 88 Zhao YL, Li YX, Ma HB et al. The screening of genes sensitive to long-term, low-level microwave exposure and bioinformatic analysis of potential correlations to learning and memory. *Biomed. Environ. Sci.* 28(8), 558–570 (2015).
- 89 Frederick AL, Saborido TP, Stanwood GD. Neurobehavioral phenotyping of G(alphaq) knockout mice reveals impairments in motor functions and spatial working memory without changes in anxiety or behavioral despair. *Front. Behav. Neurosci.* 6, 29 (2012).